Abstract

This diploma paper gives a survey of the possibilities to do optical processing and data storage with the photon echo concept, and results from experiments and numerical calculations performed within this area of research. Bitwise logical 'and' operations of two eight-bit words has been performed experimentally. Optical pulse sequences have been reemitted from a sample unchanged, reversed, compressed and expanded, and pulse sequences have been convoluted and correlated with each other experimentally by means of the photon echo process.

Table of contents

Abstract 2
Table of contents 3
1. Introduction 4
2. Purpose of the diploma work 4
3. Experimental set-up 5
    3.1. Light source 5
    3.2. The crystal 6
    3.3. Detector set-up 7
    3.4. Control electronics 7
    3.5. Pulse generation and modulation 8
4. A physical description of photon echoes 8
5. Theory of photon echoes and experimental results 9
    5.1. Theoretical description of photon echoes 9
    5.2. Two-pulse echoes 11
    5.3. Three-pulse echoes 17
    5.4. N-pulse echoes 18
    5.5. Input pulse deformation by the crystal 19
    5.6. Decay processes 20
6. Numerical calculations 22
7. Conclusions 24
8. Acknowledgements 25
9. References 26

1. Introduction

Storage and processing of information are today mostly done by computers. The upper limitations of this technology based on electronics is set by the possibilities to manufacture circuits with a very high resolution in order to squeeze in as many gates or memory cells as possible per area unit, and the inherent parasitic capacitances and inductances which limit the maximum speed at which information can be transmitted. A way to get past these problems is to use light as the information carrier instead of electrical currents. This should mean that the rate at which information can be carried is limited by the velocity and bandwidth of the optical carrier wave, which is an enormous yield in itself, as one can see from the superiority of the new optical cables as compared to the old copper cables, used in the telecommunication area. For not only transmitting information optronically but also store and process it one needs some kind of medium to assist in the interaction between data units. Several possible processes has been suggested for these purposes, among them is Persistent Spectral Hole Burning (PHB) one of the most interesting possibilities for data storage (refs. 7,9,10,12). An other process is the photon echo concept, which has been studied during this diploma work. The photon echo concept gives not only the ability to store information optronically but it also gives several powerful ways to process data in parallel, with a homogenous medium mediating the interaction between data units, that is one does not have to imprint a detailed structure in the processing medium like that needed to construct integrated circuits to be able to do processing of data. The experiments performed here hasn't used the fact that the photon echo concept only needs a small interaction volume in the three dimensional space to function, but this fact means that one could actually use not only two dimensions (as for electronic chips today) but three, to get massively parallel computing possibilities.
The photon echo concept is based on the ability of inhomogenously broadened media to remember the time dependence of an optical pulse exciting it. By exciting the sample a second time one can get a replica of the first pulse to be emitted from the sample, or under normal circumstances some kind of function of the two pulses. More complicated combinations of pulses, gives the ability to do complex processing on input data.

2. Purpose of the diploma work

Theoretical analyses of the photon echo concept for arbitrary pulse sequences has been made by e.g. W.R. Babbitt (ref. 1) as well as experimental tests of several different aspects of this concept. With these calculations as a basis for further analyses, a few interesting possibilities have been examined experimentally and numerically, and to be able to perform these experiments some fundamental characteristics of this particular experimental set-up has been measured or calculated. What really has been the primary area of research is data processing, such as logical operations on data sequences, temporal data compression and expansion, and convolution/correlation of pulse sequences with each other. Since the photon echo concept offers true parallel processing, with several sources for the input data one could easily reach processing rates of 10^6 operations per clock pulse at GHz frequencies. Many of these processes require that the optical frequency of the signal is changed continuosly during the reading/writing procedure (so called frequency chirping). Calculations and measure-

ments concerning the effect of such frequency chirps have been made. The possibilities for photon echo data storage have been analysed theoretically by P. Tidlund (ref. 3) and we have made some attempts to do experiments on data storage, but with achievements far from the theoretical predictions.

3. Experimental set-up

3.1. Light source

Between 150mW and 450mW of continuous light of a frequency equal to an absorption peak of the studied crystal was emitted from a Coherent CR-699 Ring dye laser. The appropriate wavelengh was found by observing the fluorescence light from the species at an angle perpendicular to the laser beam. By slowly (0.1-1 Hz) sweeping the wavelength of the light from the dye laser within the absorption peak, we changed the frequency range of consecutive pulse sequences and thereby decreased the deterioration of the signal due to Persistent Spectral Holeburning. The dye laser was pumped by a model 171 Ar^+-ion laser from Spectra Physics which emitted 7W to 9W multi line. The continuous dye laser light was frequency-shifted and amplitude modulated with an 1205C acousto-optic modulator from Isomet Corp. which recieved it's input RF signal from a 322B driver, and then directed at the crystal through a collimating lens.

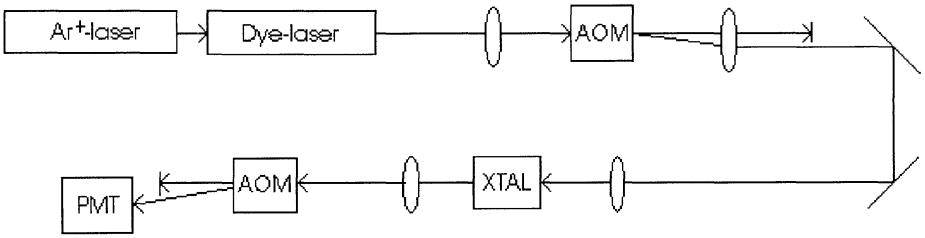

Fig.1. Experimental setup.

We originally intended to let the diffracted beam from the AOM be reflected back through the AOM and diffracted a second time, thereby causing the outcoming beam to have the same direction independently of the frequency shift in the AOM. As we had some practical problems making the two-pass set-up work in an appropriate way,

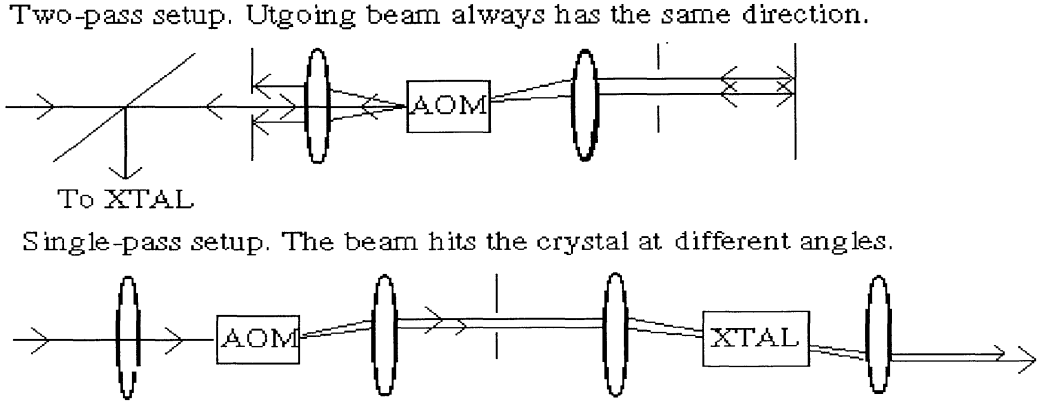

Fig. 2. AOM setup.

we did instead choose to use the single pass set-up, in despite of it's disadvantages. The used single pass set-up has got the disadvantage of emitting the output beam with a small frequency dependent displacement, which means that the beam after passing the collimating lens hits the species at the same point in space but at a slightly different angle, but this does not seem to have had an influence on the experiment. The single pass set-up also have a lower signal to background ratio, but in return it lets through a higher power.
As the echoes top amplitude has a maximum for certain values of the input pulse area (defined in section 5.1), we wanted to be able to create such pulses in a reasonably short period of time. By making the pulses longer one can increase the pulse area, but as the pulse duration gets longer, different relaxation processes are becoming more noticeable thus degrading the echoes performance. As these relaxation processes had time constants of the order of several tens of microseconds, we would like to be able to create π-pulses in about 10 μs or shorter, a requirement which was achieved.
One factor limiting the dynamic range of the measured output signal was the signal-to-background ratio. The steady state ratio was usually better than 1:1000 and was often smaller than the noise introduced by electronics, photo multiplier tube (PMT), e.t.c.

3.2. The crystal

The crystal, a Pr^{3+}:$YAlO_3$-crystal, 6.2 mm in diameter and 0.9 mm thick, doped with 0.1% Pr, was immersed in a liquid helium bath in a cryostat. It was subjected to the excitation pulses at liquid helium temperatures, and the photon-echoes were directed to the detector-part of the set-up.
The reason we performed the experiments at this temperature range (<4K) is that the photon echo phenomena in the chosen species is very short lived above approximately 20K because increasing phonon interaction in the species at higher temperatures makes the coherence decay rate increase. Accurate investigations of the coherence decay rate as a function of temperature for the material used here can be found in ref. 1. Hopefully the temperature requirements will not be this severe with the crystals we will use in proceeding experiments, if for example it would be possible to carry out experiments at liquid nitrogen temperatures this would make it easier to accomplish practically useful applications for the photon echo concept.
The transition used is that between the $^3H_4$ and the $^1D_2$ states of the Pr^+ ion at 610.53 nm. This is a transition between different $4f^2$ states of this rare earth ion, that is between states within the f-shell which is shielded from the crystalline environment by the outer 5s and 5p electrons. The f-shell is, however, only partially shielded from being influenced by the surrounding atoms and an inhomogenous broadening of the levels due to the different relative positioning of different ions gives an inhomogenous line width of this spectral line of 5 GHz. This is the frequency range available within which one can store and process data. On the other hand there is the homogenous line width acting to smear out the sharp edges of the Fourier transform of the information stored in the population distribution, thereby limiting the amount of information possible to burn into this population with a high resolution to $\Delta f_{hom}/\Delta f_{inhom}$. The homogenous line width is affected by several factors (Ref. 2) some of which can be controlled, and it is in this case around 10 kHz, making the ratio $\Delta f_{hom}/\Delta f_{inhom}=3*10^5$.

3.3. Detector set-up

To suppress the remainder of the partially absorbed excitation pulses copropagating with the photon echoes, and lower the average input signal to the PMT thereby making it possible to have a higher amplification in the PMT, the output signal from the crystal was passed through an M-AR-50 acousto-optic modulator from Soro electro-optics, with on and off switching times of 20ns and an overall input/output efficiency of 80%. It attenuated the excitation pulses with a factor of 100 to 1000 as compared to the photon echoes. This procedure demanded that the echoes were temporally separated from the excitation pulses, which was sometimes quite tricky to achieve and occasionally limited the possibilities to perform some measurements. The alternative procedure to separate the input and output pulses spatially by letting the different excitation pulses hit the species under different angles, thereby causing the echo to be emitted in yet another direction, do have the disadvantage of making the interaction volume smaller and making the experiment arrangement more complex. We therefore chose the simpler method.
The signal was then detected with a EMI 9558 QA photo multiplier tube from EMI Electron tubes. The set-ups bottleneck concerning the detected signals bandwidth was this PMT, limiting the bandwidth to about 12 MHz, as it has rise- and fall-times of about 40ns. This was not a problem though as the shortest pulses we used were of the order of hundred ns. The PMT was protected from stray light by an interference filter with a spectral width of 5 nm and a small aperture with a diameter of 200 μm. Except for the measurements of long term pulse storage and retrieval where the echoes' intensity finally got very small, the background light from lamps and windows were not a problem and the experiments could be performed at normal daylight without any need to protect the PMT from straylight.
Since the pulses during passage of the crystal were changed in shape and amplitude, we recorded the optic signal impinging on the crystal with a photo-diode for reference purposes. The final output signals from the PMT and photo-diode were both sampled with a 250MHz 2431L Digital Oscilloscope from Tektronics and then transferred to a computer through a GPIB connection.

3.4. Control electronics

The frequency sweeping of the light was controlled by a Model DS345 Synthesised function generator from Stanford Research Systems (SRS) which generated different combinations of voltage ramps, proceeded by an amplifier. The pulse generation, background signal suppression and overall synchronisation were in the different experiments controlled by several different combinations of a model DG535 Digital Delay/Pulse Generator from SRS, four computer controlled pulse generator cards SRS DG135 coupled in parallel, a 8013B Pulse Generator from Hewlett Packard giving pulse sequences consisting of several bits used in the AND experiments, and a pulse generating device manufactured at the Department of Physics.

3.5. Pulse generation and modulation

By passing the dye-laser light through the acousto-optic modulator we were able to control its amplitude and frequency. Through a TTL-input at the RF-generator generating the acoustic wave we could switch the light on and off by turning the acoustic wave on and off. This procedure gave the pulses rise- and fall-times of 30 to 50 ns.
We also frequency modulated the light, and were able to sweep the frequency up to 46MHz. The rate at which the sweeping was made, was limited by the RF-generator to a maximum of 10MHz/μs. As the sweeping of the frequency decreased the average intensity per wavelength interval, we only used sweeping rates far less than this upper limit. We had no direct way of measuring the laser lights frequency deviation from it's nominal value during the performance of an experiment, so the only estimate of this variable we got from the electric signal at the frequency modulation input to the RF-generator. As the manufacturers specifications indicate a tuning linearity of ±1% from a straight line, we have in computer simulations based on this electric signal assumed a zero deviation from linearity. Since the acoustic wave caused by the RF-generator has a velocity of 3.63 mm/μs, there is a time difference between the input electrical signals and the output optical pulses of 1μs.

4. A physical description of photon echoes

A simple description of photon echoes for the case of two excitation pulses separated τ units of time, is based on a few assumptions about the mediums response to optical pulses. The medium consist of atoms with two levels, with an energy difference between the levels described by a distribution with an average value of E. This distribution is the inhomogenous broadening. The atoms are originally all in the ground state and are excited to the upper state by a time dependent electromagnetic field, in proportion to the intensity of the field at the atoms respective nominal absorption frequencies. This means that a picture of the Fourier transform of the electromagnetic field, that is, it's frequency composition, will be burnt into the upper state population distribution. As the time after the first pulse goes by, the atoms excited to the upper state are gaining phase relative to those in the ground state, because of the time dependence of the excited state wave function

$$e^{iE_0 t/\hbar}\Psi_{upper}(\bar{r}) = e^{i\omega_0 t}\Psi_{upper}(\bar{r}) \qquad \text{(eq. 1)}$$

relative to the ground state wave function

$$\Psi_{lower} = \Psi_{lower}(\bar{r}) \qquad \text{(eq. 2)}.$$

The second pulse excites a part of the ground state population, and deexcites a part of the upper state population to the ground state. These parts, who lies after respectively before the rest of the populations in the two levels in phase, are now starting to gain, respectively loose phase relative to each other and at a time 2τ, they rephase with each other again, giving rise to an echo.
What is really causing the echo is the polarisation of the medium. The polarisation of the medium is the sum of the atomic dipole moments

$D(\bar{r},t) = \langle \Psi(\bar{r},t)|\mathrm{d}|\Psi(\bar{r},t)\rangle$ where d is the dipole operator,

that is, the polarisation is

$$P(t) = \int_V D(\bar{r},t)dr^3 \qquad \text{(eq. 3).}$$

The relation between the polarisation and the emitted lights intensity is

$$I(t) \propto |P(t)|^2 \qquad \text{(eq. 4).}$$

The reason we have mentioned that the upper states are in fact described by a distribution of frequencies, is that the upper and lower states gets in and out of phase with each other every time $\omega t = 2\pi n$, but the whole distribution of atoms with slightly different frequencies all gets in phase simultaneously at time $t = 2\tau$.
An alternative simple description of two-pulse echoes can be found in ref. 8.

5. Theory of photon echoes and experimental results

5.1. Theoretical description of photon echoes

The pulses causing the echoes are described as plane wave electromagnetic fields* :

$$E_i(t) = A_i(t)e^{i(\omega_0 t - \bar{k}\cdot\bar{r})}e^{if_i(t)t} \qquad \text{(eq. 5)}$$

where A(t) is the envelope of the field, which can be controlled electronically by amplitude modulating the pulses with e.g. an AOM. The pulses intensity is

$$I_i(t) = |E_i(t)|^2 = A_i^2(t) \qquad \text{(eq. 6).}$$

An other way of expressing a pulses ability to excite an atom is it's pulse area θ, defined as

$$\theta = dEt/\hbar \qquad \text{(eq. 7),}$$

where d is the electric dipole matrix element, E is the electric field and t the pulses duration. The pulse area tells to what extent the atoms are in the upper/lower states; if θ e.g. is equal to $\pi/2$ then the atoms are in a 50/50 superposition of the two states.
$f_i(t)$ describes the frequency modulation of the optical carrier wave. This function can also be controlled with an AOM. Throughout this work f(t) has been either zero or a linear function.
To get the absolute value of the echoes intensity one needs the absorption coefficient (Ref. 1, eq. 2.47):

$$\alpha(\omega) = \frac{4\pi^2 N g(\omega)\omega|d|^2}{\hbar c} \qquad \text{(eq. 8),}$$

where N is the number of atoms, $g(\omega)$ is the normalised inhomogenous frequency distribution ($\int_{-\infty}^{\infty} g(\omega)d\omega = 1$) and d is the atomic dipole matrix element.

---

* The physical quantity E(t) is of course the real part of the following definitions, but I haven't bothered to write that out here.

In the theoretical description of the echo phenomenon it is often convenient to use the pulses Fourier transform. The Fourier transform of a pulse is here consistently being denoted as $\Sigma_i(\omega)$, that is:

$$\Sigma_i(\omega) = \int_{-\infty}^{\infty} E_i(t) e^{-i\omega t} dt \qquad \text{(eq. 9)}$$

A few rules for Fourier transforms which are used in this work are mentioned below as a reminder:

$$\int_{-\infty}^{\infty} \Sigma_1(\omega)\Sigma_2(\omega) e^{i\omega t} d\omega = E_1(t) * E_2(t) \qquad \text{(eq. 10)},$$

where * denotes a convolution (the convolution theorem), and

$$\int_{-\infty}^{\infty} \Sigma_1^*(\omega)\Sigma_2(\omega) e^{i\omega t} d\omega = E_1(t) \otimes E_2(t) \qquad \text{(eq. 11)},$$

where $\otimes$ denotes the correlation operator. Also, a function translated relative to an other, otherwise identical function

$$E_i(t) = E_i'(t - t_i) \qquad \text{(eq. 12)}$$

has the Fourier transform

$$\Sigma_i(\omega) = e^{i\omega t_i} \Sigma_i'(\omega) \qquad \text{(eq. 13)}.$$

Another simplifying fact is that the E-fields taking part in this correlation/convolution include the factor describing the rapid oscillations at the optical signals nominal value, ω_0, but this factor can be taken out of the integral describing the echo, thus one has to deal only with the pulses amplitude and possibly its deviation from ω_0, as shown below. If the electric fields are described by a function E(t) which is a product of another function E'(t) (see eq. 5) and the part oscillating at frequency ω_0

$$E_i(t) = e^{i\omega_0 t} E_i'(t) \qquad \text{(eq. 14)}$$

then according to a standard formula for Fourier transforms

$$\Sigma_i(\omega) = \Sigma_i'(\omega - \omega_0) \qquad \text{(eq. 15)}.$$

As the echo according to section "N-pulse echoes" can be described as a product of Fourier transforms, with the terms raised to n_j (where n_j is the number of photons extracted from the E_j field) and with the number of complex conjugated terms exactly one less than the number of terms not complex conjugated then

$$E(t) = \int_{-\infty}^{\infty} \prod_j \Sigma_j^{n_j}(\omega)d\omega = \int_{-\infty}^{\infty} \prod_j \Sigma_j^{'n_j}(\omega-\omega_0)d\omega = \left[\begin{array}{l}\text{since a product of funcions of the variable} \\ \omega-\omega_0 \text{ also is a function of } \omega-\omega_0\text{, then} \\ \text{according to eqs. 14 and 15:}\end{array}\right] =$$

$$= e^{i\omega_0 t} \int_{-\infty}^{\infty} \prod_j \Sigma_j^{'n_j}(\omega)d\omega \qquad \text{(eq. 16)}$$

which shows the above statement. The above definition of the expression for the photon echo also shows that the $i\bar{k}\cdot\bar{r}$ part of the phase dependence of the pulses is not necessary to insert in the formulas because it is independent of the integration variable t, which means that the product of these e^{ikr} parts can be taken out of the integral describing the echo. As the integrand describing the echo is a product of $\Sigma_i(\omega)$ terms, where the number of complex conjugated terms exactly one less than the number of terms not complex conjugated, this product will be exactly e^{ikr} and the $i\bar{k}\cdot\bar{r}$ part can therefore be left out of the calculations.
If more information about the theory behind photon echoes and their possibilities is needed, the reader is recommended to read refs. 5,6 and 11.

5.2. Two-pulse echoes

If the two pulses have a pulse area much smaller than the area needed to saturate the transition, then according to ref. 1 the echo is described by the following integral:

$$E(t) \propto \int_{-\infty}^{\infty} \Sigma_1^*(\omega)\Sigma_2^2(\omega)e^{-i\omega t}d\omega \qquad \text{(eq. 17)}.$$

Fig. 3. Echo generated by two input pulse sequences

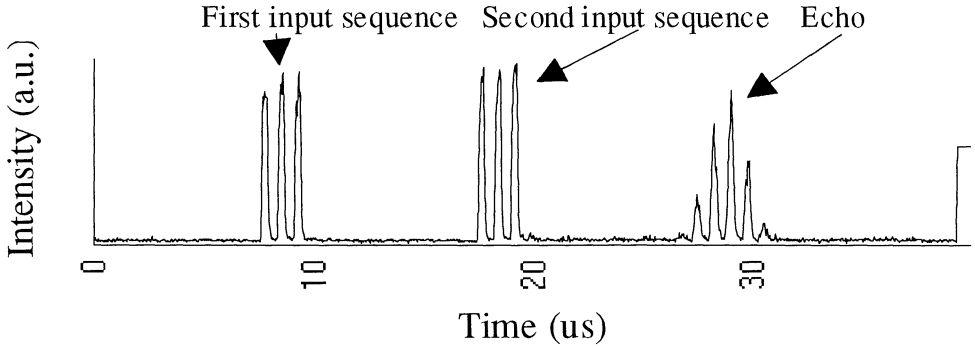

If one instead wants to look at the pulses in the time domain, one can express the above integral as the correlation of pulse one with the convolution of pulse two with itself, that is:

$$E(t) \propto E_1(t) \otimes E_2(t) * E_2(t) \qquad \text{(eq. 18)}.$$

This fact can be derived from eq. 10 and eq. 11. Figs. 3 and 4 shows a simple example of this this kind of echo formation process.

Fig. 4. Simulated echo from two input pulse sequences.

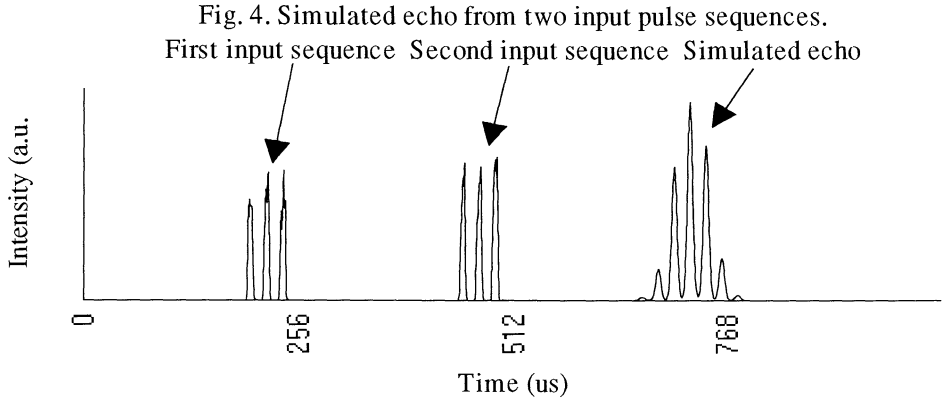

From the above Fourier integral one can see that the echo will be emitted at time $2t_2$-t_1, if one consider the following facts. Pulse one can be described as a function with it's centre around t=0 but delayed t_1, which means that the Fourier transform of the signal will be multiplied with a factor $e^{-\omega t1}$, and the same with pulse two. Mathematically this means that if functions with a prime denotes functions centred at t=0 that is

$$E_1(t) = E_1'(t-t_1) \text{ and } E_2(t) = E_2'(t-t_2) \qquad \text{(eqs. 19a,b)}$$

then

$$\Sigma_1(\omega) = e^{-i\omega t_1}\Sigma_1'(\omega) \text{ and } \Sigma_2(\omega) = e^{-i\omega t_2}\Sigma_2'(\omega). \qquad \text{(eqs. 20a,b)}$$

As the Fourier transform of pulse one is complex conjugated this term will have a positive exponent, and since the second term is being squared it's exponent will be doubled. This term affects the time dependent function by moving it's centre to $2t_2$-t_1 as shown below:

$$E(t) \propto \int_{-\infty}^{\infty} \left(e^{-i\omega t_1}\Sigma_1'(\omega)\right)^* \left(e^{-i\omega t_2}\Sigma_2'(\omega)\right)^2 e^{i\omega t} d\omega =$$

$$\int_{-\infty}^{\infty} e^{-i\omega(2t_2-t_1)}\Sigma_1'(\omega)\Sigma_2'^2(\omega)e^{i\omega t}d\omega = E'(t-(2t_2-t_1)) \qquad \text{(eq. 21)}$$

Here $E'(t) = \int_{-\infty}^{\infty} \Sigma_1'(\omega)\Sigma_2'^2(\omega)e^{i\omega t}d\omega.$

This means that if pulses one and two are separated a time τ, the echo will emanate τ after the second pulse.

If one of the pulses is approximately constant in the frequency interval over which the integral describing the echo has to be evaluated, its contribution can be taken out of the integral. If its pulse area is big enough not to let one use the linearised form of the expression one has to take into account that the echoes' electrical fields are proportional to $\sin^2\theta_2/2$ and $\sin\theta_1$ respectively, that is (acc. to ref. 1):

$$E(t) \approx \alpha L \sin(\theta_1) \int_{-\infty}^{\infty} \Sigma_2^2(\omega) e^{i\omega(t-t_1)} d\omega \approx \alpha L \theta_1 \int_{-\infty}^{\infty} \Sigma_2^2(\omega) e^{i\omega(t-t_1)} d\omega \quad \text{(eq. 22)}$$

or

$$E(t) \approx \alpha L \sin^2(\theta_2/2) \int_{-\infty}^{\infty} \Sigma_1^*(\omega) e^{i\omega(t-2t_2)} d\omega \approx \alpha L \theta_2^2/4 \int_{-\infty}^{\infty} \Sigma_1^*(\omega) e^{i\omega(t-2t_2)} d\omega =$$

$$= \alpha L(\theta_2^2/4) E_1(2t_2 - t_1 - t) \quad \text{(eq. 23)}$$

The last equality can be shown by

$$\mathrm{Re} \int_{-\infty}^{\infty} \Sigma_1^*(\omega) e^{i\omega(t-2t_2)} d\omega = \mathrm{Re}\left(\int_{-\infty}^{\infty} \Sigma_1(\omega) e^{-i\omega(t-2t_2)} d\omega \right)^* = \mathrm{Re}\, E_1^*(2t_2 - t_1 - t) = E_1(2t_2 - t_1 - t) \quad \text{(eq. 23a)}$$

Here L is the sample length. This means that under these circumstances in the first of the above cases the echo will be a time reversed replica of the first pulse, delayed 2τ. Since the echo for these two-pulse echoes will be delayed a period of time equal to the time that has passed since the first pulse, it is not a practical way to recall the stored information, but it does at least show the possibilities of the photon echo concept.

The following results from an echo experiment with two square wave pulses, shows how the echoes' dependence of the contributing pulses take three different forms as the pulse areas are changed. In fig. 5 pulse area one is held constant and small, in fig. 6 pulse area two is being held constant and small. The pulse areas were controlled by changing the pulses duration, t_1 and t_2, and the area is proportional to the duration.

Fig. 5. Peak intensity, t1 constant.

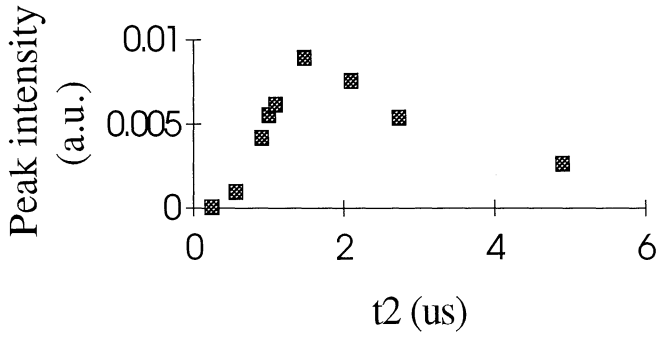

In the small signal interval the echoes peak intensity is proportional to $(\theta_2/2)^4$ and θ_1^2, respectively, since in these cases

$$I(t) \propto |E(t)|^2 \approx \sin^4(\theta_2/2) \left| \int_{-\infty}^{\infty} \Sigma_1^*(\omega) e^{i\omega t} dt \right|^2 \approx \theta_2^4/4 \left| \int_{-\infty}^{\infty} \Sigma_1^*(\omega) e^{i\omega t} dt \right|^2 \quad \text{(eq. 24)}$$

or

$$I(t) \propto |E(t)|^2 \approx \sin^2(\theta_1)\left|\int_{-\infty}^{\infty}\Sigma_2^2(\omega)e^{i\omega t}dt\right|^2 \approx \theta_1^2\left|\int_{-\infty}^{\infty}\Sigma_2^2(\omega)e^{i\omega t}dt\right|^2 \qquad \text{(eq. 25)}.$$

As the small signal interval is exceeded, diagrams 5 and 6 instead show $\sin^4(\theta_2/2)$- and $\sin^2(\theta_1)$dependence, as predicted by theory.
As the pulse areas grow even more, depending on the long duration of the respective pulses, none of the above approximations (eqs. 24, 25) can be used due to relaxation processes (see section 5.6).

Fig. 6. Peak echo intensity, t2 constant.

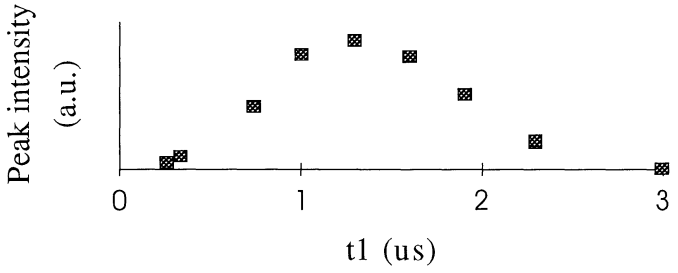

Fig. 7. 8+8 bit AND operation.

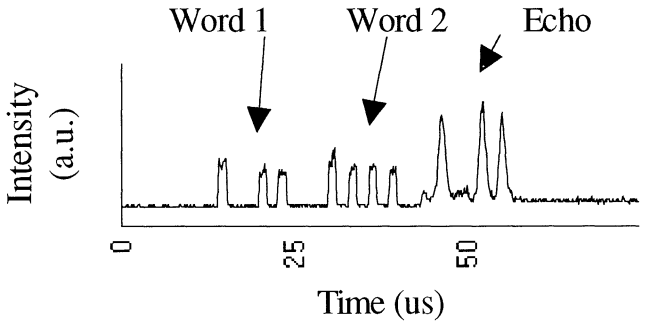

An other interesting feature of the two-pulse echo is the fact that if one defines the presence of light as a binary "one" and the absence as a "zero", it can work as a logical AND function. Two pulses give rise to an echo, and no other combination of "ones" and "zeroes" does, just as the AND function is defined. ANDing more than one pair of binary variables does demand that the individual digits in a binary number don't interfere with any other bits than the corresponding digit in the other number. A way of achieving this is by giving the different digits different frequencies. This can be done by chirping the frequency of the laser light as the different bits are written into the sample, and performing an identical chirp during the second word. We did this experimentally with four and eight bits, as is shown in fig. 7.

Fig. 8. Max intensity of echo for two chirped input pulses, as a function of chirping rate.

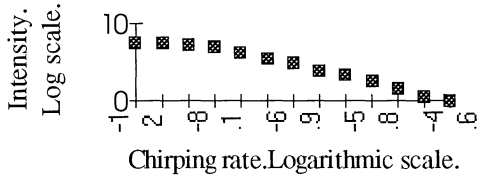

The constraint on the sweeping ratio as compared to the ANDed pulses lengths is that the pulses' widths in the frequency plane must be smaller than the frequency difference between succeeding bits. If the frequency width of a square pulse is approximated by $4/\tau$, where τ is the pulse width, and the frequency is swept at a speed of a Hz/s then this constraint can be expressed as $a>4/\tau^2$. (The difference in frequency between two pulses is $a\tau$, and since $a\tau$ must be $>4/\tau$ then $a>4/\tau^2$). Unfortunately, for constant

bit energy the echoes intensity decreases rapidly as the sweeping rate is increased according to both computer simulations and experimental data, so the only possibility to AND many bits is to spread them out temporally. In fig. 8 results from numerical calculations is presented showing the echo intensity decay with increasing chirping rate. The upper limit to this solution are the dephasing times T_1, and T_2, which has limited the number of bits to about 20 in our experiments.

Fig. 9. Compression of three bit pulse sequence.

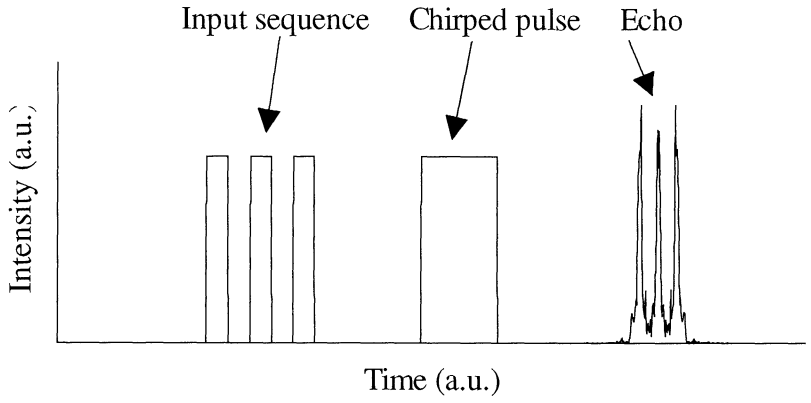

If the first pulse-sequence is swept as described above, but the second is swept at a different speed (and constantly held "on", see fig. 9) the output signal will be a compressed respectively expanded version of pulse one, depending on whether the sweeping rate is higher (compression) or lower (expansion). A great deal of distortion is though added with this simple companding* method, and we didn't manage to perform it experimentally with a good signal to noise ratio until after the completion of the experimental part of this diploma work, so only computer simulations of these operations are presented here. If pulse sequence one is T long and the second pulse is aT, and swept within the same frequency interval as the first then the echo will be (2a-1)T long, as long as the frequency sweeping rate is fast enough to allow a one to one correspondence between the frequency intervals contributing to the echo. This means that if a=1 the echo is as long as the first pulse; if it's in the range $\frac{1}{2} \leq a < 1$ the echo will be a compressed version of the first pulse and if a>1 it will be expanded. If a is exactly ½ then all the frequencies contributing to the echo will contribute to the echo at the same instant and give rise to a pulse of high intensity. If $a < \frac{1}{2}$ the echo will be a reversed version of the input pulse sequence. (Simple algebra shows the above statement. If pulse one is T long, starting at t=0 and pulse two is aT, starting at time t=S, then the echo start at t=2S and ends at t=2(S+aT)-T. The echoes' duration will be (2a-1)T.). Figures 9 and 10 show pulses companded with this method.

* A 'compander' is an electronic circuit capable of compressing or expanding the dynamic range of an input signal. The word companding is used here as a synonym for 'expanding or compresssing a signal temporally'.

Fig. 10. Expansion of three bit pulse sequence.

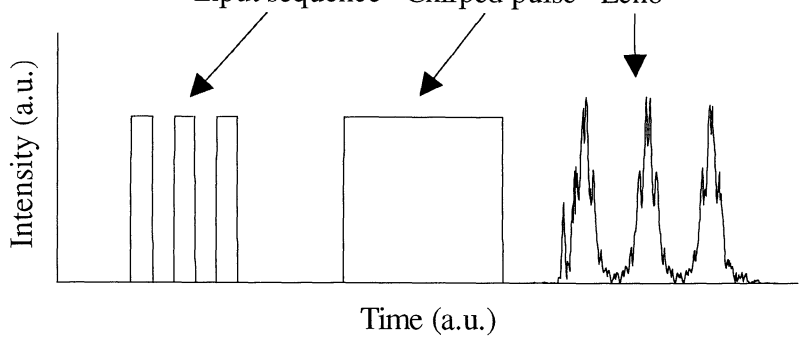

Fig. 11. Echo from one short pulse and one chirped pulse.

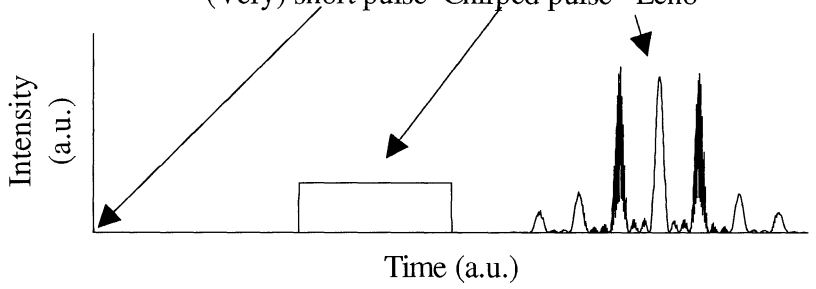

An other interesting feature of the photon echo concept is the possibility to look at the fingerprint of a pulses Fourier transform in the population distribution and through that get indirect information of it's time-dependence, even if the pulse itself is too short, temporally, to be detected with a high temporal resolution (see fig. 11). By letting the short pulse excite the medium and then reading it out with a second swept pulse, pulse one can be reconstructed from the echo with knowledge about the behaviour of the second pulse. Pulse two must be swept over a frequency interval larger than 2/t, where t is pulse ones width, and as can be seen from the convolution integral, the echo will have a duration approximately equal to twice the length of pulse two and start at time 2τ, where τ is the time difference between pulse one and pulse twos beginning. As the inhomogenous broadening of the medium in this case is of the order of gigaherz one could reconstruct the time dependence of pulses as short as parts of nanoseconds even though the electronic equipment used in the experiment limits the upper time resolution to tenths of nanoseconds. This should in principle be applicable to even shorter pulses for media with an even broader inhomogenous line width and a dephasing time long enough to let one sweep over this broader interval with unchanged sweeping rate. Organic molecules often have inhomogenously broadened absorption peaks with a width of the order of teraherz, theoretically making it possible to reconstruct pulses with a time resolution of less than picoseconds. This method has the advantage to e.g. streak cameras that it can see in two dimensions spatially.

5.3. Three-pulse echoes

Fig. 12. Three pulse echo.

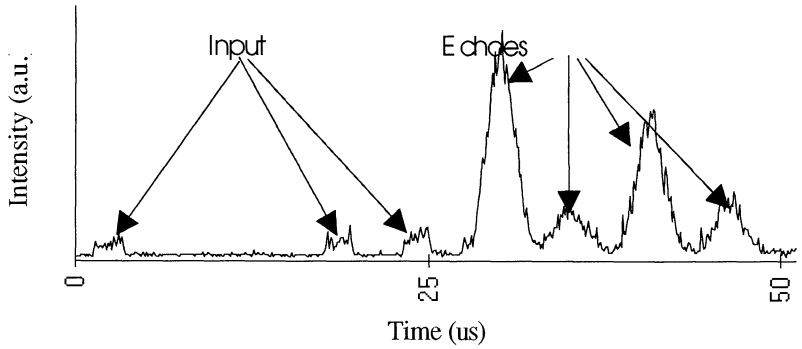

In the case of three exciting pulses, four echoes are emitted (fig. 12). One is caused by pulses one and two, the other by pulses two and three, the third by pulses one and three, and the fourth is a stimulated echo caused by all three pulses. Here we are only interested in the three-pulse echo and neglect the two-pulse echoes. If the pulses occur at times t_1,t_2 and t_3, the echo is emitted at $t=t_3+t_2-t_1$, as can be seen from a calculation similar to that in section "two-pulse echoes". By arranging the pulses temporally in a suitable fashion, one can see to that the different echoes don't overlap. For pulses with an energy much smaller than the energy needed to saturate the species, the following equation holds for the emanating echo (ref. 1):

$$E(t) = \frac{2|p|^2 \alpha L}{\hbar^2} \frac{1}{2\pi} \int_{-\infty}^{\infty} \Sigma_1^*(\omega)\Sigma_2(\omega)\Sigma_3(\omega) e^{i\omega t} d\omega \qquad \text{(eq. 26)}.$$

Fig. 13. Read pulse + echo of the word 1010101010101010.

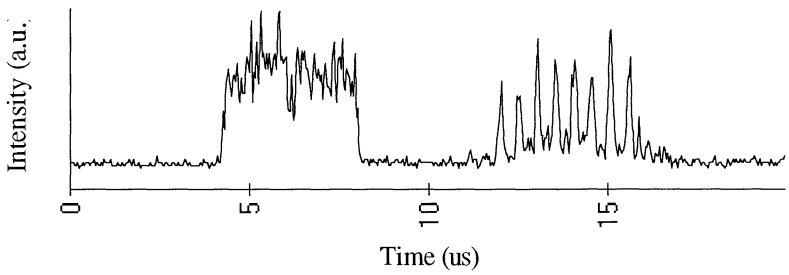

If the product of two of the pulses' Fourier transforms is approximately constant within the frequency interval the Fourier transform of the third pulse is to be integrated over, this product can be taken out of the integral. If the pulses' pulse areas are small enough, one can approximate the influence of these Fourier transforms by their respective pulse areas, otherwise one has to consider the echoes non linear dependence on the pulse areas, in a fashion equal to the one used in section "two pulse echoes". E.g. if the product of pulses two and three is approximately constant over the frequency interval that the transform of pulse one is appreciably large then

$$E(t) \propto \sin(\theta_2)\sin(\theta_3) E_1(-(t-(t_3+t_2-t_1))) \qquad \text{(eq. 27)}$$

There are two possible ways of making a pulses Fourier transform approximately constant within a certain frequency interval. One is to make the pulse short enough, thus obtaining a Fourier transform approximately constant over a broad range. The other is to linearly sweep the pulses frequency around its nominal value. In this work the second method was used consistently throughout the experiments.

The Fourier transform of the pulse remaining in the integral, causes the echo to become shaped as this pulse, but time-reversed if the transform is complex conjugated. This means, that the shape of this pulse is remembered by the sample, and it can be read out from the sample at any time, not considering decay processes mentioned in 5.6. Experimentally, we have only managed to resolve a pulse sequence consisting of twenty-two bits in the echo, and here we present a figure of the sixteen output data bits preceded by the third, read pulse (fig. 13). This output pulse sequence is preceded by a first, swept, write pulse, and a second pulse consisting of sixteen input data bits. Difficulties to produce write and read pulses short and intense enough to make the echo a copy of the input sequence, caused us to choose to sweep these pulses' frequencies instead but this also has the disadvantage of limiting the number of bits that can be resolved to about the value calculated for multiple bit logical ANDing.

5.4. N-pulse echoes

We haven't had any reason to use pulse sequences consisting of more than three pulses during these experiments, but the formula for the echo from N pulses, where N is odd, is presented here for completeness:

$$E(t) \propto \int_{-\infty}^{\infty} \Sigma_1^*(\omega)\Sigma_2(\omega)\Sigma_3^*(\omega)\Sigma_4(\omega)\cdots\Sigma_{N-2}^*(\omega)\Sigma_{N-1}(\omega)\Sigma_N(\omega)e^{i\omega t}d\omega \qquad \text{(eq. 28)}$$

One sees from the above formula that the echo will emanate at $t=t_N+(t_{N-1}-t_{N-2})+..$ $..+(t_4-t_3)+(t_2-t_1)$. One also sees that the number of complex conjugated terms is exactly one less than the number of terms that are not complex conjugated, a fact that have already been used. Echoes are also formed for every permutation of the subscripts, provided that the new $t>t_N$.

time eliminated this problem, but since the echo decreases exponentially with an initial decay rate of 4-10 μs^{-1}, the echo/background ratio has a maximum when the echo occurs a few tens of μs after the last excitation pulse.
Beat oscillations sometimes appears in the output signal, and this phenomenon has two quite different causes, which might take on a similar appearance. By exciting the medium by a square pulse, with a rapid change in light frequency during the pulse, the output signal from the crystal right after the change in frequency will be a mixture of the FID light induced by the first part of the pulse, and the light from the second part of the pulse. These two light sources, both coherent and with a narrow frequency distribution, will as they are mixed give rise to a beat oscillation in the signal with a frequency equal to the change in frequency during the pulse (fig. 15). This means that the beat frequency is continuously variable, which is not the case for the second phenomenon.
This second phenomenon has it's origin in the hyperfine structure of both the ground state and the excited state. These two levels are in this case both split in three hyperfine levels, with different splittings (see fig. 16), where all three ground state sub levels are about equally populated. The selection rules for the F quantum number (ΔF=0) gives three possible transition frequencies between the ground and excited state hyperfine levels. Thus an input signal which has a broad enough frequency distribution, can excite atoms between two or more combinations of these levels giving rise to beats in the FID light and the echoes.

Fig.16. Hyperfine structure of $Pr^{+3}YAl^{3}O$

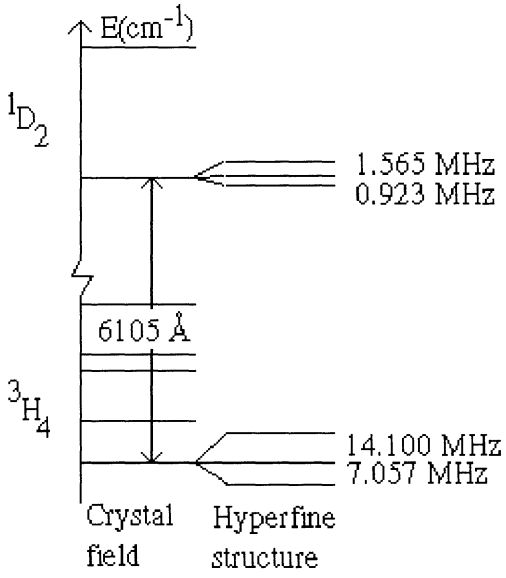

5.6. Decay processes

Initially we have discarded all relaxation and homogenous decay processes that may diminish the echo intensity. It is a reasonable approximation to do so as long as certain constraints which will be defined are fulfilled, but in the general case it has to be taken into account. The homogeneous relaxation time T_2, has two different kinds of effects on the echoes. It acts to smooth out the copy of the Fourier transform burned into the population distribution, by convoluting it with a distribution function representing the effect of the homogenous decay time. This means that details in the transform can't be resolved with a resolution higher than about $\gamma=1/T_2$. I the time plane this means that pulses longer than T_2 will be distorted, as can be seen from figs. 5,6. If, however, the pulses lengths don't exceed T_2, one can choose to discard this effect. The terms $\Sigma_i(\omega)$ in the equations describing the echo (eqs. 17,21-26,28) should therefore be replaced by

$\Sigma_i(\omega) * D(\omega)$ (eq. 29)

where

$$D(\omega) = \int_{-\infty}^{\infty} e^{-\gamma|t|} e^{i\omega t} dt = \frac{2\gamma}{\gamma^2 + \omega^2} \quad \text{(eq. 30)}$$

and the integral for the inverse Fourier transform multiplied with a
$e^{-\gamma t}$
term. The other effect of the relaxation processes is that the coherences that are the origin of the photon echoes are decreasing with time. Even if the pulse duration is $<T_2$, one has to take into account that during the periods between the pulses the coherences will decrease exponentially. Only if the whole pulse sequence don't exceed T_2, one can totally discard this effect.
The mechanism mentioned above is the reason why fig. 5 looks the way it does. As the length of pulse two increases the pulse area should increase linearly, the $e^{-\gamma t}$ term makes the pulse area asymptotically go towards a finite value, and this is why the curve seems to end at a constrant value instead of oscillating in a sine-like fashion.
The mechanisms affecting the homogenous relaxation time are the lines natural lifetime which here is long relative to other effects and not possible to influence; phonon interactions in the crystal which are temperature dependent, interaction between excited atoms, frequency drift of the laser and nuclear spin flips due to spin flips among the surrounding atoms. This last effect can be suppressed by applying an external magnetic field to the species, thereby breaking the degeneracy of hyperfine levels with oppositely directed nuclear spins. A fourth, yet not fully explained mechanism, seems to have a pulse intensity dependence (refs. 4,15) and has been suggested to arise from optical density effects or instantaneous spectral diffusion.
The natural relaxation processes affects the optical coherences, just by diminishing the number of atoms in the upper state, thereby cancelling the valleys in the ground state population distribution with the peaks in the excited state population distribution. One would think that the atoms relaxing back to the ground state from the upper state with a half intensity time T_1, should mean that the peaks in the upper state population distribution would exactly cancel the valleys in the ground state distribution. There does though exist a possibility ε that the atoms relaxing will end up in a different hyperfine structure level than they were originally excited from, thereby leaving a part of the population distribution burned into the ground state unaffected. The fact that the atoms relaxes back through several different other levels increases the possibility for such a change of the hyperfine structure level, and it has in this particular case been calculated to ε=0.066 (ref. 3 p. 26 and ref. 14). This initial relaxation process then leaves the ground state population unaffected after a few T_1, which in this material is 180 μs.

Fig. 17. Initial relaxation rate.

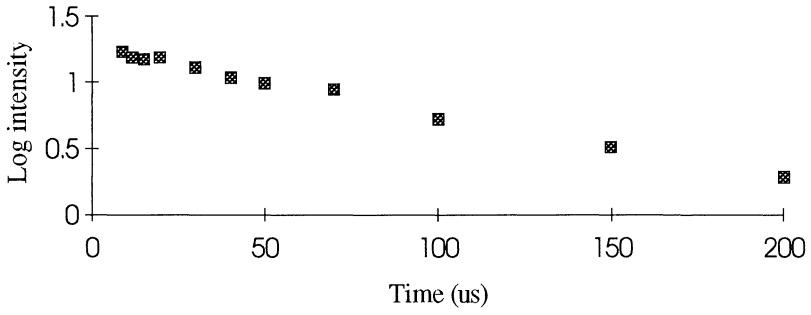

The relaxation processes directly affecting the optical coherence decay, are not those that limits the possibilities for long term storage of information (ref. 2), but sets the

upper limit to how detailed the copy of the pulses' Fourier transform can be resolved. This decay time, T_2, is in the material used in these experiments about 10 μs and it increases rapidly with temperature. A measurement of the echoes maximum intensity as a function of the time between pulses two and three, for a three pulse case, initially showing an exponential decay of the intensity with a decay time of T_1, and asymptotically showing a decay time of T_{relax}, where T_{relax} is defined as the inverse of the sum of all contributing relaxation processes affecting the echo, is presented in figure 17. As indicated by the above discussion the decay should look like this:

$$E(t) \propto e^{-2\Delta_{12}/T_2}\left((1-\varepsilon^2)e^{-\Delta_{23}/T_1} + \varepsilon^2 e^{-\Delta_{23}/T_{relax}}\right) \qquad \text{(eq. 32)},$$

where Δ_{ij} is the time between pulses i and j.

6. Numerical calculations

For the computer simulations I have used the program Mathcad on different PC-compatible computers. Several properties of the real world optical signals have had to be "guessed", linearly interpolated from experimental data or ignored. Noisy parts of experimental data, which according to our intentions are supposed to be zero, have been replaced by the value zero, a procedure which shouldn't affect the simulated results otherwise than to lowering the background noise level. Also, known properties of the crystal which affects the output signal, like it's time- and intensity dependent absorption coefficient, FID from the exciting light pulses, the effect of the homogenous dephasing time and it's hyperfine structure affecting the output, have been neglected in order to make computations easier. Several deficiencies of the properties of the laser light, which were not possible to measure directly like phase- and frequency noise, have been neglected as well.
As the Rabi solution indicates (for a derivation of this, see e.g. ref. 13), the integral expressions describing the echoes are not linearly dependent on the input signals. Throughout these simulations we have used the linearised versions of these expressions, which in some cases might explain differences between calculated and measured results, since we during the experiments have tried to maximise the input pulses intensity and not to keep them within the linear regime.
The calculated signals are not to scale and I have not tried to get accurate information of the absolute intensities of the echoes, only about their temporal dependence.
The discrete fast Fourier transform algorithm used for the calculations require that the bandwidth of the transformed signal is less than half the sampling rate. The data taken from the oscilloscope is supposed to be low pass filtered to fulfil this demand, but concerning information about the frequency shift which we have added to the signal afterwards, we had to take care of this demand separately. The curves from the oscilloscope showing the pulses' amplitude, had to be multiplied with an sinusoidal term describing the sweeping of the frequency. This term oscillates at up to the frequency at^2, where a is the sweeping rate and t the duration of the pulse, and we had to see to that this frequency didn't exceed the limits. Describing pulses swept at a high rate and/or with a long duration, put high demands on the computing speed and the capacity of the math program.
To get an estimation of the differences between simulated and measured echoes in a more complex case I present in fig. 18 experimental data from an experiment where one chirped input pulse is followed by two three-pulse input sequences, and the echoes caused by these input pulse sequences. The output is consisting of three

groups of pulses with declining intensity, due to the effects of relaxation processes. The fourth echo (a two-pulse echo caused by input pulses one and two) emanates between input pulses two and three and can not be seen in this scale. By eliminating one input pulse sequence at a time, one can experimentally determine which parts of the echo belongs to which input pulses. Numerically one has to calculate the different echoes separately, add the contributions to the output electric field and then take the absolute square of it to get the intensity. Even though I have used an approximation of the lowest possible order, one can see that this gives quite good results (fig. 19).

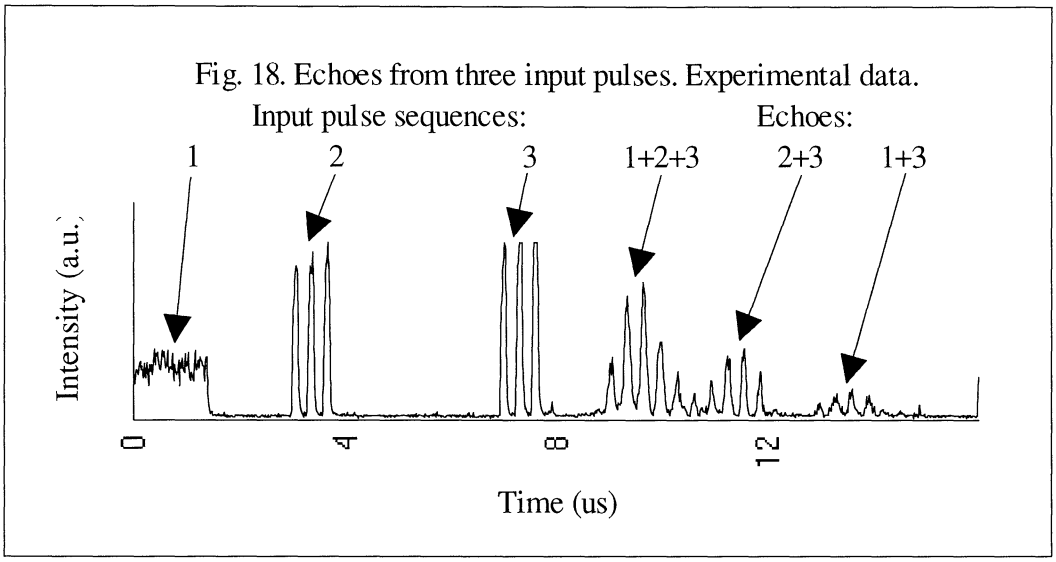

Fig. 18. Echoes from three input pulses. Experimental data.

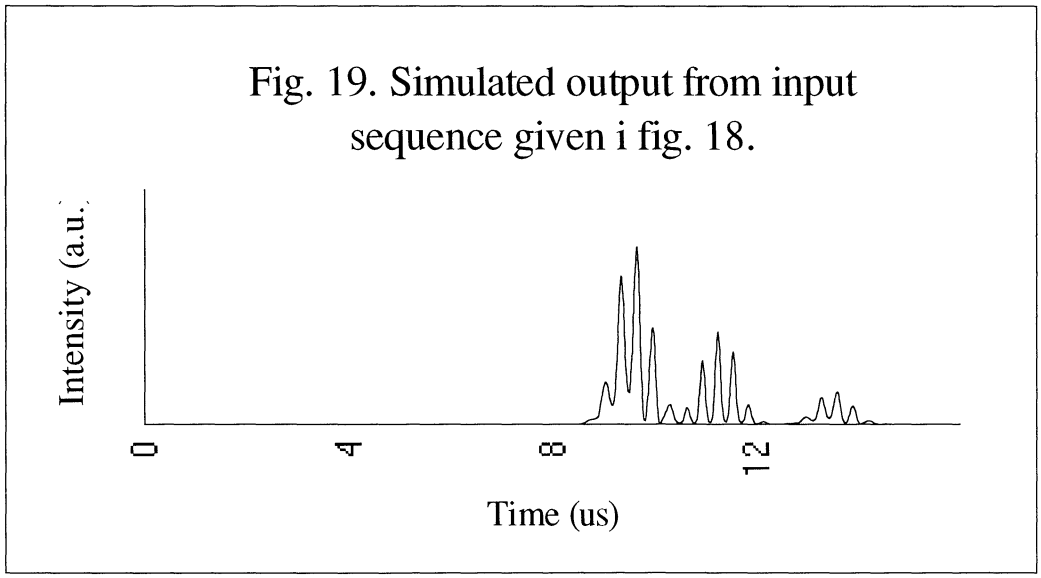

Fig. 19. Simulated output from input sequence given i fig. 18.

7. Conclusions

As has been shown in this diploma work, the photon echo concept is a very promising candidate for future optical processing units or optical memories, in some form. A few of the simplest data processing possibilities have been performed experimentally with reasonably good results, and some interesting aspects of the concept has been analysed analytically and numerically, which has given a few promising ideas for proceeding investigations. One way to perform the logical operation 'and' by chirping the frequency of the input optical signal during write of the two words to be 'and':ed has been tried out experimentally for word lengths of up to sixteen bits. This method for performing logical operations on several proceeding bits has also been studied numericallly considering number of bits per time interval depending on the chirping rate and the effects limiting the total number of bits possible to 'and' have been studied. The results indicate that in the crystal used for the experiments logical operations on words of lengths equal to commonly used word lengths used in computers are easily achieved with a good signal to noise ratio.
An interesting method for temporally compressing or expanding an input pulse sequence has been studied mainly numerically, giving a means of expanding /compressing pulse sequences and, at least theoretically, a possibility to resolve the time dependence very short pulses using reasonably slow detecting equipment.

8. Acknowledgements

I would like to thank my instructor Dr. Stefan Kröll for the help he has given me during the experiments, and all hints concerning the theoretical aspects of this diploma work. I also would like to thank Prof. Sune Svanberg who initiated my interest in this project and has given me a possibility to continue my research on this topic. Finally, I would like to thank the staff at the Department of Atomic Physics for their help and encouragement, and my girl friend for coping with me and my formulas like eq. 28 during this project.

9. References

Ref.1 "The response of inhomogenously broadened optical absorbers to temporally complex light pulses", W.R. Babbit, PhD thesis, Harvard University, Cambridge, Mass. 1987.

Ref.2 "Stimulated photon echo & photon echo relaxation measurements", S. André, Diploma work, LRAP - 124, Lund 1991.

Ref.3 "Material considerations for time domain optical storage", P. Tidlund, Diploma work, LRAP - 131, Lund 1992.

Ref.4 "Influence of excited-state Pr^{3+} on the relaxation of the Pr^{3+}:$YAlO_3$ $^3H_4$-$^1D_2$ transition", S. Kröll, E. Y. Xu and R. Kachru, Phys. Rev., Vol. **44**, (1991) 30-34.

Ref.5 Information erasing in the phenomenon of long-lived photon echo", Akhmediev, Optics Lett., Vol. **15**, (1990) 1035-1037.

Ref.6 "Frequency-chirped copropagating multiple-bit stimulated-echo storage and retrieval in Pr^{3+}:$YAlO_3$", S. Kröll, L. E. Jusinski and R. Kachru, Optics Lett., Vol. **16**, (1991) 517-519.

Ref.7 "Can single-photon processes provide useful materials for frequency-domain optical storage?", W. E. Moerner and M. D. Levenson, J. Opt. Soc. Am., Vol. **2**, (1985) 915- 924.

Ref.8 "Understanding optical echoes using Schrödingers equation: I. Echoes excited by two optical pulses", A. V. Durrant, J. Manners and P. M. Clark, Eur. J. Phys. Vol. **10**, (1989) 291-297.

Ref.9 "Technological aspects of frequency domain data storage using persistent spectral hole burning", F. M. Schellenberg, W. Lenth and C. Björklund, App. Opt., Vol. **25**.

Ref.10 "Gated spectral hole-burning for frequency domain optical recording", Lenth and W. E. Moerner, Optics Comm., Vol. **58**.

Ref.11 "Coherent time-domain optical memory", R. Kachru and D. L. Huestis, SRI Int. Research Proposal No. PYC 85-097.

Ref.12 "Frequency domain optical storage", G. C. Bjorklund and G. Castro, Research Report, IBM Research Laboratory, San Jose, California, 95193.

Ref. 13 "Laser Physics", M. Sargent, M. O. Scully, W. E. Lamb, Addison-Wesley Publishing Company, 1974.

Ref. 14 "Optical-pumping effects on Raman-heterodyne-detected multipulse rf nuclear-spin-echo decay", L. E. Erickson, National Research Council, Ottawa, Ontario, Canada, Phys. Rev. B, Vol. **42**, (1990), 3789-3797.

Ref. 15 "Intensity-dependent photon-echo relaxation in rare-earth-doped crystals", S. Kröll, E. Y. Xu, M. K. Kim, Phys. Rew. B, Vol. **41**, (1990), 11568-11571.